Can Surface Soil Moisture Information Identify Evapotranspiration Regime Transitions?

Jianzhi Dong[1,2] ![ID], Ruzbeh Akbar[1] ![ID], Daniel J. Short Gianotti[1] ![ID], Andrew F. Feldman[3,4] ![ID], Wade T. Crow[5] ![ID], and Dara Entekhabi[1,6] ![ID]

[1]Department of Civil and Environmental Engineering, Massachusetts Institute of Technology, Cambridge, MA, USA, [2]Institute of Surface-Earth System Science, Tianjin University, Tianjin, China, [3]Biospheric Sciences Laboratory, NASA Goddard Space Flight Center, Greenbelt, MD, USA, [4]NASA Postdoctoral Program, NASA Goddard Space Flight Center, Greenbelt, MD, USA, [5]United States Department of Agriculture, Agricultural Research Service, Hydrology and Remote Sensing Laboratory, Beltsville, MD, USA, [6]Department of Earth, Atmospheric and Planetary Sciences, Massachusetts Institute of Technology, Cambridge, MA, USA

Abstract The transition of evapotranspiration between energy- and water-limitation regimes also denotes a nonlinear change in surface water and energy coupling strength. The regime transitions are primarily dominated by available moisture in the soil, although other micro-meteorological factors also play a role. Remotely sensed soil moisture is frequently used for detecting evapotranspiration regime transitions during inter storm dry downs. However, its sampling depth does not include the entire soil profile, over which water uptake is dominated by plant root distribution. We use flux tower, surface (θ_s; observations at 5 cm), and vertically integrated in situ soil moisture (θ_v; 0–50 cm) observations to address the question: Can surface soil moisture robustly identify evapotranspiration regime transitions? Results demonstrate that θ_s and θ_v are hydraulically linked and have synchronized evapotranspiration regime transitions. As such, θ_s and θ_v capture comparable statistics of evapotranspiration regime prevalence, which supports the utility of remote-sensing θ_s for large-scale land-atmosphere exchange analysis.

Plain Language Summary During dry down periods between storms, soil moisture availability can be a limiting factor for evapotranspiration (water-limited regime). In contrast, evapotranspiration is insensitive to soil moisture for adequately wet conditions, and is primarily determined by atmospheric evaporative demand (energy-limited regime). During interstorm drydowns, the landscape changes from one regime to another. The timing of evapotranspiration regime change signifies a change in the coupling of landscape water and energy balances. Soil moisture based on microwave remote sensing has been frequently used for analyzing global-scale evapotranspiration regime transitions. However, microwave signals are mainly sensitive to surface soil moisture (θ_s), which is not directly a sampling of root water uptake from the deeper soil profile. Therefore, the applicability of remotely sensed θ_s information for evapotranspiration regime identification is uncertain. In this study, we use flux tower, surface (θ_s, observations at 5 cm) and vertically integrated (θ_v, 0–50 cm) in situ observations to examine the reliability of θ_s for evapotranspiration regime identification. Results demonstrate that θ_s and θ_v are equivalently skillful for identifying evapotranspiration regime changes and the time a landscape spends in the water-limited regime. Therefore, remotely sensed θ_s can be used to robustly analyze evapotranspiration regime changes and the associated large-scale land-atmosphere exchanges.

1. Introduction

Soil moisture is the primary variable controlling land surface water and energy balance coupling (Dirmeyer et al., 2000; Entekhabi et al., 1996). Specifically, during extended periods without precipitation, soil moisture falls below a threshold value—leading to a transition from energy- to water-limited evapotranspiration regimes (Feldman et al., 2020; Haghighi et al., 2018; Seneviratne et al., 2010). Under water-limited regimes, evapotranspiration is reduced with decreased soil moisture, which results in increased sensible heating of the lower atmosphere (Berg et al., 2014; Seneviratne et al., 2010). As a result, the transitions between different evapotranspiration regimes regulate the development of the boundary layer at hydrometeorological timescales and the onset of heatwaves on hydroclimatological timescales (Feldman et al., 2019; Koster et al., 2019; Yuan et al., 2019).

Passive microwave remote sensing (radiometry) is used for sensing soil moisture dynamics at the global scale (Entekhabi et al., 2010; Kerr et al., 2010; Wagner et al., 1999). These data sets allow—for the first time—a global

view of soil moisture dynamics, enabling identification of global distributions and transitions between energy- and water-limited evapotranspiration regimes. For example, Denissen et al. (2020) uses the merged multi-satellite European Space Agency Climate Change Initiative soil moisture product and FluxCOM evapotranspiration data set to quantify the spatial distribution of the threshold soil moisture values over Europe. Likewise, Crow et al. (2015) combine multisensory soil moisture and evapotranspiration products to estimate the overall coupling strength of evapotranspiration and soil moisture, which implicitly reflects the occurrence frequency of water-limited regimes at a given location. This method is further employed for diagnosing numerical weather forecasting systems (Crow et al., 2020), land surface models (Dong et al., 2020), and Earth system models (Dong et al., 2022). Recently, Akbar, Gianotti, et al. (2018) demonstrate that L-band retrieved soil moisture drydown patterns can be decoded to quantify daily evapotranspiration regime transitions. This approach is noteworthy since it only uses soil moisture data, which relaxes the requirement for high-quality evapotranspiration data. Their soil moisture drydown analysis has been recently extended to the global scale and applied to flash drought monitoring (Sehgal et al., 2021a, 2021b).

All of these studies are based on remote sensing soil moisture measurements that have, at best, a sampling depth of less than ~10 and ~5 cm more typically (Njoku & Kong, 1977; Ulaby et al., 1978). They are thus essentially analyzing land-atmosphere coupling processes using only the dynamics of surface soil moisture (θ_s). However, plant roots can reach to soil water storages at several tens of centimeters and for certain limited species, to tens of meters (Fan et al., 2017; Gao et al., 2014; Yang et al., 2016). Therefore, evapotranspiration can draw water from soil layers that are considerably deeper than the θ_s sampling depth (Buitink et al., 2020; Green et al., 2019; Humphrey et al., 2021; Li et al., 2021). Based on this line of reasoning, the expectation is that θ_s is likely biased in its representation of evapotranspiration regime transitions or overall land surface energy partitioning (Hirschi et al., 2014; Mueller & Seneviratne, 2012). Indeed, a recent study shows that θ_s-based thresholds of soil moisture for separating energy and water limited regimes (denoted as θ_*) are biased low versus those for root zone soil moisture (Buitink et al., 2020).

In contrast, recent studies argue that θ_s and root zone soil moisture temporal dynamics are tightly correlated due to their hydraulic connectivity (Akbar, Short Gianotti, et al., 2018; Albergel et al., 2008; Dong & Crow, 2018; Short Gianotti et al., 2019) and, hence, tend to reflect similar surface energy balance information (Qiu et al., 2016, 2020).

Therefore, a natural question is whether evapotranspiration regime transitions are evident in remotely sensed θ_s. Specifically, is deeper soil moisture information absolutely necessary to correctly identify the evapotranspiration regime transitions?

In order to address this question, we take an observation-driven approach to assess evapotranspiration regime transitions (as deduced from flux tower measurements and in situ soil moisture sensors) based on θ_s (measured at 5 cm depth) and a vertically integrated profile soil moisture (θ_v, from 0 to 50 cm profile). We quantify the degree of consistency in evapotranspiration regime transitions based on these two soil moisture series at sites in the continental United States. In this way, we provide observational evidence for the consistency of θ_s- and θ_v-based evapotranspiration regime transitions and clarify the utility of remotely sensed surface soil moisture for large-scale land-atmosphere exchange analysis.

2. Data and Method

Water- and energy-limited evapotranspiration regimes are identified based on volumetric soil water content (θ) and a threshold value θ_*, that is, as $\theta < \theta_*$ and $\theta \geq \theta_*$, respectively. Approaches for determining θ_* and evapotranspiration regime transitions are outlined in Sections 2.1 and 2.2. Our analysis is entirely based on in situ observations. Given the general data availability, this study uses 0–50 cm vertically integrated soil moisture (θ_v) to represent root zone temporal dynamics. There are, of course, exceptions where certain plants have adapted to frequent water stress by extending roots into far deeper soil layers and approaching underground aquifers (Fan et al., 2017; Gao et al., 2014). Nonetheless, for most ecosystems, more than 75% of vegetation roots are located in the top 50 cm of the soil column (Zeng, 2001), and soil moisture availability above 30 cm is most responsible for vegetation dynamics (Li et al., 2021). Therefore, θ_v is expected to be representative of the general vegetation root water stress conditions.
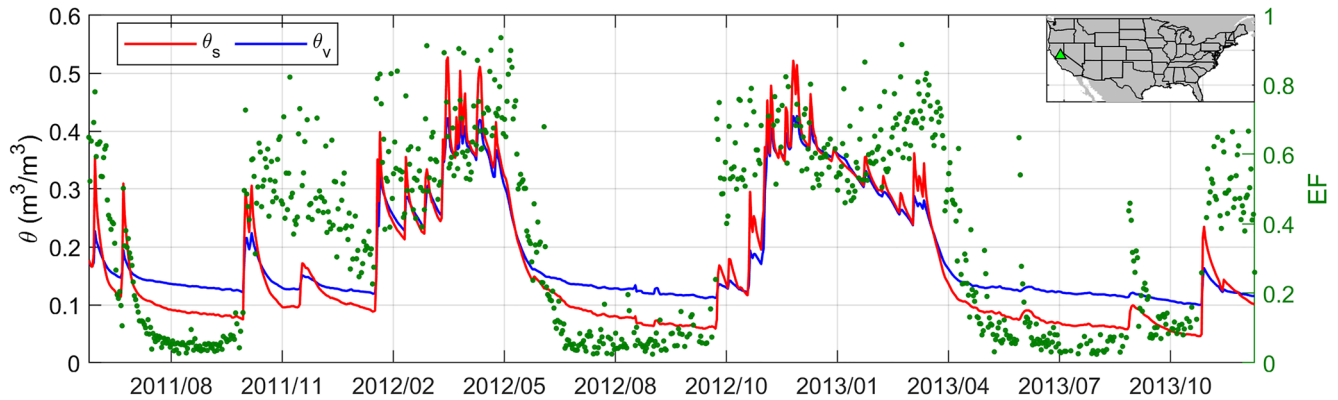
Figure 1. Example time series of θ_s and θ_v, and evaporative fraction (EF) at the US-Ton site (Ma et al., 2016). The location of US-Ton site is shown in the upper right map. Due to the relatively complete soil moisture profile measurement, flux tower and soil moisture observations for the woody savanna land cover type are used here for demonstration.

As noted above, to demonstrate the robustness of our findings, two independent approaches are employed for θ_* determination. The first approach is based on turbulent fluxes measured by eddy-covariance systems and high-quality soil moisture profile observations (Section 2.1). The second approach is based on soil moisture drydown analysis alone (Akbar et al., 2018), which can be extended to, far more numerous, soil moisture in situ measurement locations lacking colocated flux towers.

2.1. Flux-Tower Based ET Regime Identification

Land surface partitioning of available energy for exchange with the overlying atmosphere can be characterized using the non-dimensional evaporative fraction (EF)

$$EF = \frac{LE}{LE + SH} \tag{1}$$

where LE and SH are daily mean latent and sensible heat fluxes (W/m^2), respectively. Clearly, EF values are unstable when its denominator is close to zero. Therefore, only days with both LE and SH values greater than 1 W/m^2 are considered in this study.

EF is affected by a number of environmental factors, but soil moisture status dominates the day-to-day EF variations, especially in water-limited locations (Lu et al., 2016). Contrasting EF sensitivities to soil moisture variations are evident in the energy-limited ($\theta \geq \theta_*$, zero slope) and water-limited ($\theta < \theta_*$, positive slope) regimes (Dirmeyer et al., 2000; Haghighi et al., 2018; Lu et al., 2016). Therefore, the threshold θ_* can be identified by fitting a piece-wise linear function to the observed θ-EF relationship. Once the θ_* value is determined, the temporal transitions of different ET regimes can be identified according to the variations of θ with respect to θ_*.

Observations from the AmeriFlux US-Ton site (38.43°N−120.96°W, see Figure 1 inset) located in California are used here for demonstration (Ma et al., 2016). This site is selected because it provides high-quality LE, SH, and soil moisture profile observations (available at 5, 20, and 50 cm depths for the woody savanna site) throughout the extended 2000–2020 period. More importantly, this site is characterized by a Mediterranean climate with frequent evapotranspiration regime transitions. In addition, dry-wet transitional climate conditions are typically associated with strong temporal variations in rooting depth, which maximize the difference of θ_s- and θ_v-characterized vegetation water availability (Fan et al., 2017; Gao et al., 2014). Therefore, this site is ideal for rigorously testing the consistency of θ_s- and θ_v-identified evapotransption regimes. Note that the US-Ton site has observations for both grass and wood savanna land cover types. However, only top 20 cm soil moisture values are measured for the grass site and hence, we focus on observations from the woody savanna.

We acknowledge that the US-Ton site is not representative of woody forest and humid climate conditions. However, as mentioned above, forest sites with complete soil moisture profile (top 50 cm) observations are very limited. In addition, humid regions dominated by energy-limited regimes have limited value for characterizing the evapotranspiration regime fluctuations. Nonetheless, evapotranspiration regime analysis based on various land

cover types and climate conditions are comprehensively analyzed based on high-quality soil moisture networks in the following section.

2.2. Evapotranspiration Regime Identification From Soil Moisture Drydown Analysis

Soil moisture losses on nonprecipitation days are dominated by water- and energy-limited evapotranspiration, and drainage dominated hydrological regimes, which can be quantified as a piecewise linear function (Laio et al., 2001). Therefore, once the functional form of soil moisture losses has been optimized, the associated θ_* values are also implicitly determined. In this study, the soil moisture drydown analysis is performed using the existing framework proposed by Akbar, Gianotti, et al. (2018).

Soil moisture profile observations from Soil Climate Analysis Network (SCAN) and U.S. Climate Reference Network (USCRN) are used for soil moisture loss analysis. Likewise, measurements at the 5 cm and 0–50 cm averaged daily soil moisture values are used for representing θ_s and θ_v temporal dynamics, respectively. We limit ourselves to sites with at least 5 years of available measurements during the 2010–2021 period. In addition, given θ_s is theoretically more sensitive to meteorological forcing (Albergel et al., 2008), sites with θ_v standard deviations higher than that of θ_s are excluded. Overall, 114 stations are used and their spatial distributions are shown in Figure 3.

To minimize the impact of seasonal variations in vegetation and climate on soil moisture losses (Feldman et al., 2019; Haghighi et al., 2018; Sehgal et al., 2021b), soil moisture drydown analyses are performed separately for each season. Note that θ_* cannot be estimated for sites dominated by either water- or energy-limited regimes. Figure S1 in Supporting Information S1 shows the stations that do not consistently reflect both regimes and, therefore, cannot be used to estimate θ_*.

Soil moisture loss analysis requires high-quality precipitation data to identify dry down time series. To do so, we use the global, daily 0.1-degree Multi-Source Weighted-Ensemble Precipitation product (Beck et al., 2019). This product combines gauge-based, remote-sensing, and reanalyzed precipitation estimates. Therefore, it is more accurate than traditional gridded precipitation estimates over the continental US.

2.3. The Consistency of θ_s and θ_v Identified Evapotranspiration Regimes

To evaluate the general consistency of θ_s- and θ_v-based evapotranspiration regime identification, two metrics are used. The first metric is the probability of $\theta \leq \theta_*$ (denoted as γ), which quantifies the incidence of the water-limited regime

$$\gamma = n_w/n \tag{2}$$

where n_w is the number of days when θ is lower than θ_* (i.e., water-limited regime) and n is the total number of days with valid observations. The θ_s- and θ_v-based γ values are calculated on site-by-site bases for each season, which are subsequently used for quantifying the consistency of θ_s- and θ_v-based evapotranspiration regime identification.

In addition, a consistency metric π is defined and used to compare θ_s and θ_v estimated evapotranspiration regimes, calculated as

$$\pi = n_c/n \tag{3}$$

where n_c is the number of days that θ_s and θ_v identify the same evapotranspiration regime. Clearly, π ranges from zero to one, and $\pi = 1$ indicates that θ_s and θ_v are identical in regime identification.

3. Results and Discussions

3.1. Flux Tower-Based Analysis

Figure 1 shows an example times series of observed EF, θ_s, and θ_v. The demonstration is for a 2 year sub-sample of the 20 years of US-Ton flux tower and soil moisture sensor data. As expected, θ_s and θ_v dry-wet temporal variabilities are tightly correlated (Short Gianotti et al., 2019). As a result, both θ_s and θ_v can capture similar
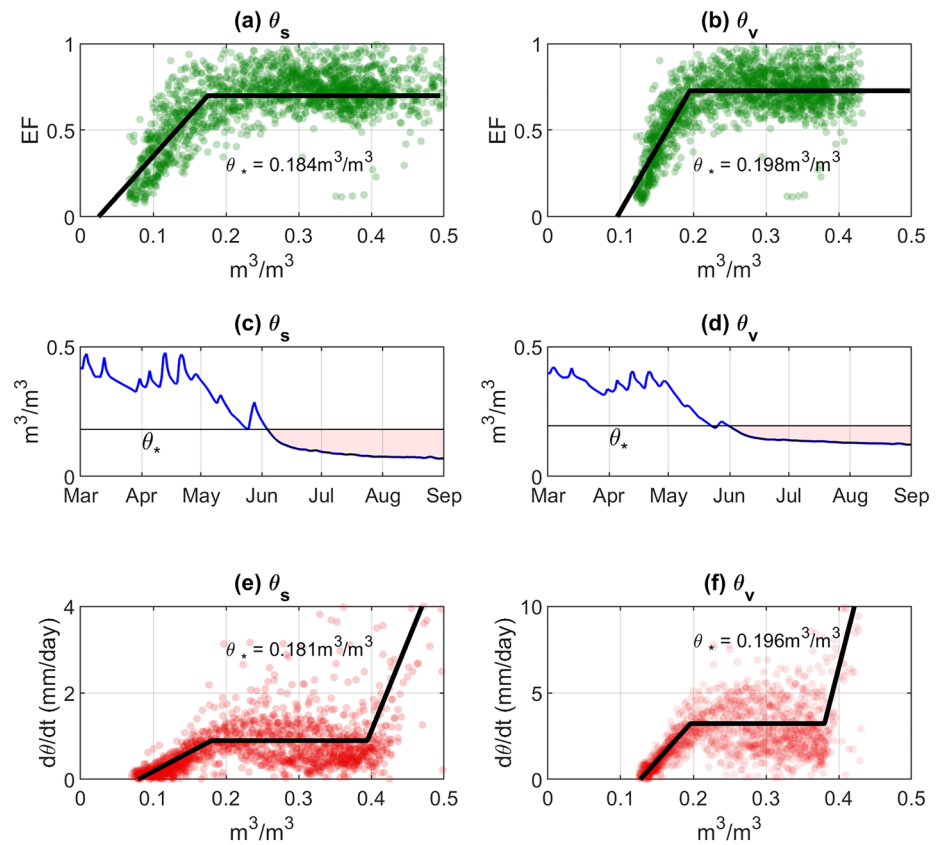
Figure 2. Evaporative fraction (EF) as a function of θ_s (a) and θ_v (b) at the Tonzi Ranch (US-Ton) example site. Parts (c) and (d) are θ_s- and θ_v-based evapotranspiration regime classification from March 2010 to September 2010 (with red shadings denote the water-limited regime), respectively. The θ_* values, estimated solely based on soil moisture temporal dynamics via dry down analysis, are shown in parts (e) and (f). Observations during 2000–2020 March-April-May months are used for the θ_* analysis (i.e., parts a, b, e and f), with thick black lines indicating optimized hydrological regimes (Section 2.1).

intra- and inter-seasonal variations of EF—reflecting the time-varying control of soil moisture on land surface energy partitioning.

Interestingly, it is at least visually evident that θ_s can be better suited in capturing the short-term EF variations, compared to θ_v. For instance, sharply increased EF is observed in September 2013—suggesting an increase in evapotranspiration water availability. Such evapotranspiration water availability change is clearly captured by θ_s, but not by θ_v. This may suggest that θ_s is the primary water source for soil evaporation and canopy transpiration at this site, and subsurface soil moisture has limited evapotranspiration information. As a result, integrating soil moisture information from deeper soil layers may even degrade evapotranspiration information contained in θ_s. This finding is consistent with a recent flux tower-based study, which demonstrates that θ_s tend to contain higher EF information than that of θ_v, even sampled across various climate and vegetation conditions (Qiu et al., 2020).

Figure 2 provides a quantitative comparison of θ_s- and θ_v-based evapotranspiration regime identification for the site shown in Figure 1. The scatterplot of observed θ_s and EF demonstrate a clear nonlinear relationship, which signifies the transition of water- and energy-limited evapotranspiration regimes as a function of soil water availability (Figure 2a). Based on this θ_s-EF relationship, the optimal θ_* can be determined and used for quantifying the temporal variations of evapotranspiration regimes, defined as θ_{s*} (Figure 2a). Relative to θ_s, θ_v contains lower temporal dynamics and is typically wetter in dry months (Figure 1). Therefore, θ_{v*} is higher than that of θ_{s*} (Figure 2b), which is consistent with a previous study (Buitink et al., 2020).

However, the degree to which θ_s and θ_v capture the same evapotranspiration regime transitions (with π approaching 1) depends not only on the absolute value of the soil moisture threshold θ_*, but also on the marginal probability distribution of the corresponding soil moisture time series. It is clear that both θ_* values and the statistical
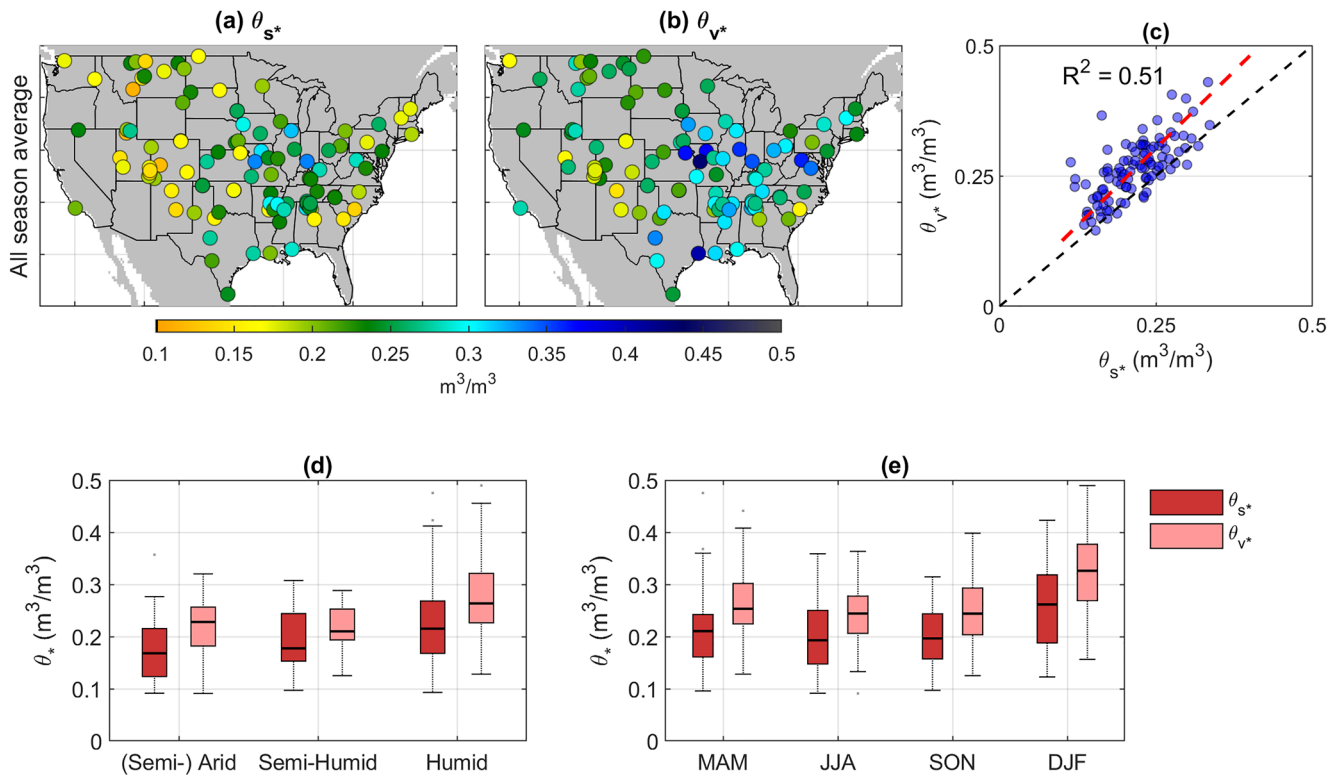
Figure 3. Spatial distribution of θ_s- and θ_v-based θ_* estimates, denoted as θ_{s*} and θ_{v*}, respectively (parts a and b). The spatial consistency of θ_{s*} and θ_{v*} is shown in c, with each symbol denoting θ_* estimates from a particular site. Red dashed line in part c denotes the relationship of θ_{s*} and θ_{v*} based on total least squares linear regression (slope is 1.18 and the intercept is 0.0076 m³/m³). The impacts of local climate and seasonality on θ_* are shown in parts d and e, respectively. Note that both θ_{s*} and θ_{v*} are estimated separately for each season and all-season-averages are presented in parts (a–d). The (Semi-) Arid, Semi-Humid, and Humid climate zones are classified as land areas with aridity index (calculated as the ratio of annual mean precipitation and potential evapotranspiration) lower than 0.5, 0.5–0.65, and higher than 0.65, respectively.

distributions of θ_s and θ_v are different. Ultimately, the question is whether landscape evapotranspiration regimes identified by θ_s and θ_v are mutually consistent?

To address this question, Figures 2c and 2d provide an illustrative example of θ_s- and θ_v-based regimes identification. They show that θ_s and θ_v are equivalent in terms of capturing the onset and the development of evapotranspiration water stress, that is, the transition from an energy-to water-limited regime (see the red shaded area). As sampled across the entire 2000–2020 period, the binary consistency (π) of θ_s- and θ_v-based regimes classification is 0.97. Therefore, it appears that although θ_s and θ_v time series contain systematic differences, their evapotranspiration regime identification is consistent. This implies a generally shape-preserving transformation between surface and column-average soil moisture dynamics at the daily timescale (Short Gianotti et al., 2019).

3.2. Soil Moisture Drydown Based Evapotranspiration Regime Identification

Soil moisture dry down analysis based evapotranspiration regime identification is illustrated in Figures 2e and 2f using the same US-Ton site. The three segments of the piecewise linear function (defined by the state-dependent loss rate of $d\theta/dt$ and θ) denote the water- and energy-limited evapotranspiration and drainage dominated hydrological regimes, respectively. It is noteworthy that θ_* derived from θ-EF relationship and dry down analysis are highly consistent (compare reported θ_* values in Figures 2a and 2e as well as Figures 2b and 2f). Comparisons of these two methods at additional sites can be found in Figure S2 in Supporting Information S1. These results suggest that soil moisture drydown analysis is a viable tool for evapotranspiration regime identification.

Figure 3 shows θ_* estimates over 114 soil moisture sites. For brevity, we focus on the seasonal average of θ_* estimates, and the temporal variability of θ_* is shown in Figure 3e. Both θ_{s*} and θ_{v*} demonstrate a clear west-east gradient (Figures 3a and 3b), which reflects climatic influence on θ_* (Figure 3d). The geographic distributions
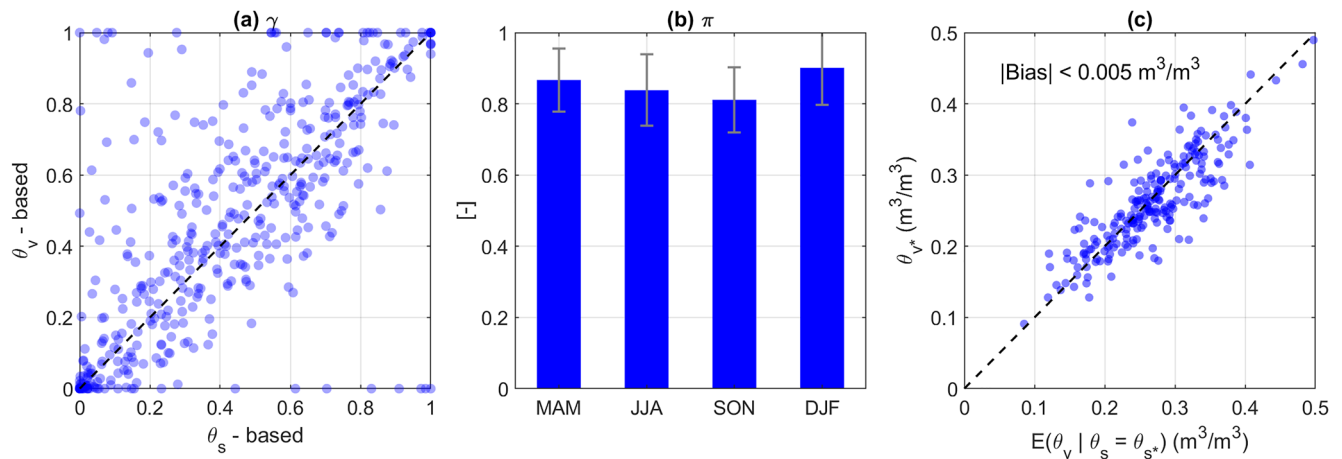
Figure 4. The consistency of θ_s- and θ_v-based evapotranspiration regime identification as evaluated using both γ (a) and π (b). γ is the fraction of time spent in the water-limited regime (integrating the moisture threshold and marginal distribution). π quantifies the consistency of θ_s- and θ_v-identified day-to-day evapotranspiration regime transition. Note that part a includes γ values from all seasons and all sites. Error bars in part b denote the standard deviation of π across all available sites for a particular season. Part c shows the comparison of θ_* directly estimated by θ_v drydown analysis (i.e., θ_{v*}) and conditionally averaged θ_v when θ_s reaches θ_{s*}.

of θ_{s*} and θ_{v*} are highly consistent, with a spatial correlation of 0.71 (coefficient of determination $R^2 = 0.51$, Figure 3c). However, there is a shift (bias) between θ_{s*} and θ_{v*} as evident in Figure 3c—indicating transitions typically occurring at lower θ_s and higher θ_v contents.

Although θ_* values and temporal dynamics contain systematic differences, θ_s- and θ_v-based evapotransparition regimes are highly consistent. Across all seasons and all sites, the correlation of θ_s- and θ_v-based γ (the incidence of water-limited regime) is 0.72 and the relative difference is 8.5% (Figure 4a). Likewise, the spatially averaged binary consistency (π) of θ_s- and θ_v-based evapotranspiration regime classification also exceeds 0.8 for all four seasons (Figure 4b). Given the uncertainties in soil moisture observations (Chen et al., 2016) and θ_* estimation (Akbar, Gianotti, et al., 2018), the consistency of θ_s- and θ_v-based results are remarkable. Therefore, it appears that θ_* adjusts to the amplitude of soil moisture dynamics, which yields consistent evapotranspiration regime identification based on either θ_s or θ_v.

Figure 4c provides a candidate explanation for the observed consistency between θ_s and θ_v-based evapotranspiration regime identification. The soil moisture profile during dry downs starts to deplete from the surface layer, due to the dual action of bare soil evaporation and transpiration by shallow roots near the surface (see Figure 1). Therefore, during inter-storm dry downs, the onset of water stress should start from the surface and first become evident in the θ_s time series. At this time, subsurface soil layers are likely still under the energy-limited regime. Therefore, the start of the energy- to water-limited regime transition of the soil profile is determined by the time when θ_s drops to θ_{s*}. The question is if the hydraulic connectivity in the profile results in a nearly synchronized transition of θ_v to its threshold value (i.e., θ_{v*}) as well.

The consistency that the transitions are closely coupled for the surface and the integrated profile can be quantified by assessing how close is θ_v to its threshold θ_{v*} at the time θ_s reaches its threshold θ_{s*}, that is, whether $\theta_{v*} = E(\theta_v | \theta_s = \theta_{s*})$?

Figure 4c shows that $E(\theta_v | \theta_s = \theta_{s*})$ and θ_v drydown analysis estimated θ_{v*} are highly consistent and unbiased. This directly explains why θ_s- and θ_v-based evapotranspiration regime identification is so highly consistent.

Note that Figure 4 is not representative of cases with strongly decoupled surface and subsurface soil moisture dynamics (Scott et al., 2008). For instance, cases where θ_s is constantly dominated by water-limited regimes, whereas θ_v indicates a wet and energy-limited regime (see Figure S1 in Supporting Information S1). For those cases, θ_s may be a better indicator of evapotranspiration regime—given that θ_v cannot capture the water stress of soil evaporation or vegetation roots in the surface soil layer. Likewise, in nature, site-dependent layered pedology, xeric plants with deep root taps, macropores and groundwater dynamics may complicate the connections of surface and subsurface hydraulic links (Kramer & Boyer, 1995). However, these conditions may be only

applicable to very limited cases, given that θ_s and θ_v are broadly consistent in their classification of evapotranspiration regime transitions (Figures 2 and 4).

4. Conclusion

Transitions between water- and energy-limited evapotranspiration regimes are the building blocks for large-scale land-atmosphere interaction, which, for example, have direct implications for hydroclimate extremes (e.g., heatwave and flash drought). Remotely sensed surface soil moisture information is now available at the global scale and has been used for such analysis. However, due to its limited representativeness of the soil moisture profile, the reliability of remotely sensed surface soil moisture for land-atmosphere coupling analysis remains undefined. Here, we use observation-driven approaches based on in situ soil moisture profile and flux tower observations to address the applicability of surface soil moisture for identifying the evapotranspiration regimes. As such, we seek to provide theoretical support for the application of remotely sensed surface soil moisture in large-scale hydroclimatological and hydrometeorological analyses.

Based on the soil moisture—EF relationship and a soil moisture drydown analysis, we demonstrate that surface (at 5 cm, θ_s) and vertically integrated (0–50 cm, θ_v) soil moisture measurements are consistent in regards to their evapotranspiration regime classification. This is because the θ_s is preferentially dried by evapotranspiration during drydowns. Hence, θ_s determines the onset of evapotranspiration water stress and regime transitions. Therefore, the θ_s and θ_v dynamics essentially provide mutually useful information for quantifying evapotranspiration regime changes. Although this conclusion may be violated by cases with complex surface-subsurface hydraulic links, it is supported and verified by a range of in situ observations across a range of climate, soil and vegetation conditions.

As such, we demonstrate that surface soil moisture, equivalent to that now available globally from Earth-orbiting satellites (with over a decade of data), contains sufficient and reliable information for identifying landscape evapotranspiration regimes. Therefore, it highlights the value of remotely sensed soil moisture for monitoring the onset and the development of hydroclimate extremes, and its applicability for large-scale land-atmosphere interaction analysis.

Data Availability Statement

The in situ soil moisture observations are available at: https://www.geo.tuwien.ac.at/insitu/data_viewer/ and https://www.ncei.noaa.gov/pub/data/uscrn/products/daily01/. The AmeriFlux data are available at: https://ameriflux.lbl.gov/data/data-availability/.

References

Akbar, R., Gianotti, D. J. S., McColl, K. A., Haghighi, E., Salvucci, G. D., & Entekhabi, D. (2018). Estimation of landscape soil water losses from satellite observations of soil moisture. *Journal of Hydrometeorology*, *19*(5), 871–889. https://doi.org/10.1175/jhm-d-17-0200.1

Akbar, R., Short Gianotti, D., McColl, K. A., Haghighi, E., Salvucci, G. D., & Entekhabi, D. (2018). Hydrological storage length scales represented by remote sensing estimates of soil moisture and precipitation. *Water Resources Research*, *54*, 1476–1492. https://doi.org/10.1002/2017wr021508

Albergel, C., Rüdiger, C., Pellarin, T., Calvet, J. C., Fritz, N., Froissard, F., et al. (2008). From near-surface to root-zone soil moisture using an exponential filter: An assessment of the method based on in-situ observations and model simulations. *Hydrology and Earth System Sciences*, *12*, 1323–1337. https://doi.org/10.5194/hess-12-1323-2008

Beck, H. E., Wood, E. F., Pan, M., Fisher, C. K., Miralles, D. G., Van Dijk, A. I. J. M., et al. (2019). MSWEP V2 global 3-hourly 0.1 precipitation: Methodology and quantitative assessment. *Bulletin of the American Meteorological Society*, *100*, 473–500. https://doi.org/10.1175/bams-d-17-0138.1

Berg, A., Lintner, B. R., Findell, K. L., Malyshev, S., Loikith, P. C., & Gentine, P. (2014). Impact of soil moisture–atmosphere interactions on surface temperature distribution. *Journal of Climate*, *27*, 7976–7993. https://doi.org/10.1175/jcli-d-13-00591.1

Buitink, J., Swank, A. M., van der Ploeg, M., Smith, N. E., Benninga, H.-J. F., van der Bolt, F., et al. (2020). Anatomy of the 2018 agricultural drought in the Netherlands using in situ soil moisture and satellite vegetation indices. *Hydrology and Earth System Sciences*, *24*, 6021–6031. https://doi.org/10.5194/hess-24-6021-2020

Chen, F., Crow, W. T., Colliander, A., Cosh, M. H., Jackson, T. J., Bindlish, R., et al. (2016). Application of triple collocation in ground-based validation of soil moisture active/passive (SMAP) level 2 data products. *IEEE Journal of Selected Topics in Applied Earth Observations and Remote Sensing*, *10*, 489–502. https://doi.org/10.1109/JSTARS.2016.2569998

Crow, W. T., Gomez, C. A., Sabater, J. M., Holmes, T., Hain, C. R., Lei, F., et al. (2020). Soil moisture–evapotranspiration overcoupling and L-Band brightness temperature assimilation: Sources and forecast implications. *Journal of Hydrometeorology*, *21*, 2359–2374. https://doi.org/10.1175/jhm-d-20-0088.1

Crow, W. T., Lei, F., Hain, C., Anderson, M. C., Scott, R. L., Billesbach, D., & Arkebauer, T. (2015). Robust estimates of soil moisture and latent heat flux coupling strength obtained from triple collocation. *Geophysical Research Letters*, *42*, 8415–8423. https://doi.org/10.1002/2015gl065929

Denissen, J. M. C., Teuling, A. J., Reichstein, M., & Orth, R. (2020). Critical soil moisture derived from satellite observations over Europe. *Journal of Geophysical Research: Atmospheres*, *125*, e2019JD031672. https://doi.org/10.1029/2019jd031672

Dirmeyer, P. A., Zeng, F. J., Ducharne, A., Morrill, J. C., & Koster, R. D. (2000). The sensitivity of surface fluxes to soil water content in three land surface schemes. *Journal of Hydrometeorology*, *1*, 121–134. https://doi.org/10.1175/1525-7541(2000)001<0121:tsosft>2.0.co;2

Dong, J., & Crow, W. T. (2018). Use of satellite soil moisture to diagnose climate model representations of European soil moisture-air temperature coupling strength. *Geophysical Research Letters*, *45*, 12–884. https://doi.org/10.1029/2018gl080547

Dong, J., Dirmeyer, P. A., Lei, F., Anderson, M. C., Holmes, T. R. H., Hain, C., & Crow, W. T. (2020). Soil evaporation stress determines soil moisture-evapotranspiration coupling strength in land surface modeling. *Geophysical Research Letters*, *47*, e2020GL090391. https://doi.org/10.1029/2020gl090391

Dong, J., Lei, F., & Crow, W. T. (2022). Land transpiration-evaporation partitioning errors responsible for modeled summertime warm bias in the central United States. *Nature Communications*, *13*, 1–8. https://doi.org/10.1038/s41467-021-27938-6

Entekhabi, D., Njoku, E. G., O'Neill, P. E., Kellogg, K. H., Crow, W. T., Edelstein, W. N., et al. (2010). The soil moisture active passive (SMAP) mission. *Proceedings of the IEEE*, *98*, 704–716. https://doi.org/10.1109/jproc.2010.2043918

Entekhabi, D., Rodriguez-Iturbe, I., & Castelli, F. (1996). Mutual interaction of soil moisture state and atmospheric processes. *Journal of Hydrology*, *184*, 3–17. https://doi.org/10.1016/0022-1694(95)02965-6

Fan, Y., Miguez-Macho, G., Jobbágy, E. G., Jackson, R. B., & Otero-Casal, C. (2017). Hydrologic regulation of plant rooting depth. *Proceedings of the National Academy of Sciences*, *114*, 10572–10577. https://doi.org/10.1073/pnas.1712381114

Feldman, A. F., Short Gianotti, D. J., Trigo, I. F., Salvucci, G. D., & Entekhabi, D. (2019). Satellite-based assessment of land surface energy partitioning–soil moisture relationships and effects of confounding variables. *Water Resources Research*, *55*, 10657–10677. https://doi.org/10.1029/2019wr025874

Feldman, A. F., Short Gianotti, D. J., Trigo, I. F., Salvucci, G. D., & Entekhabi, D. (2020). Land-atmosphere drivers of landscape-scale plant water content loss. *Geophysical Research Letters*, *47*, e2020GL090331. https://doi.org/10.1029/2020gl090331

Gao, H., Hrachowitz, M., Schymanski, S. J., Fenicia, F., Sriwongsitanon, N., & Savenije, H. H. G. (2014). Climate controls how ecosystems size the root zone storage capacity at catchment scale. *Geophysical Research Letters*, *41*, 7916–7923. https://doi.org/10.1002/2014gl061668

Green, J. K., Seneviratne, S. I., Berg, A. M., Findell, K. L., Hagemann, S., Lawrence, D. M., & Gentine, P. (2019). Large influence of soil moisture on long-term terrestrial carbon uptake. *Nature*, *565*, 476–479. https://doi.org/10.1038/s41586-018-0848-x

Haghighi, E., Short Gianotti, D. J., Akbar, R., Salvucci, G. D., & Entekhabi, D. (2018). Soil and atmospheric controls on the land surface energy balance: A generalized framework for distinguishing moisture-limited and energy-limited evaporation regimes. *Water Resources Research*, *54*, 1831–1851. https://doi.org/10.1002/2017wr021729

Hirschi, M., Mueller, B., Dorigo, W., & Seneviratne, S. I. (2014). Using remotely sensed soil moisture for land–atmosphere coupling diagnostics: The role of surface vs. root-zone soil moisture variability. *Remote Sensing of Environment*, *154*, 246–252. https://doi.org/10.1016/j.rse.2014.08.030

Humphrey, V., Berg, A., Ciais, P., Gentine, P., Jung, M., Reichstein, M., et al. (2021). Soil moisture–atmosphere feedback dominates land carbon uptake variability. *Nature*, *592*, 65–69. https://doi.org/10.1038/s41586-021-03325-5

Kerr, Y. H., Waldteufel, P., Wigneron, J.-P., Delwart, S., Cabot, F., Boutin, J., et al. (2010). The SMOS mission: New tool for monitoring key elements of the global water cycle. *Proceedings of the IEEE*, *98*, 666–687. https://doi.org/10.1109/jproc.2010.2043032

Koster, R. D., Schubert, S. D., Wang, H., Mahanama, S. P., & DeAngelis, A. M. (2019). Flash drought as captured by reanalysis data: Disentangling the contributions of precipitation deficit and excess evapotranspiration. *Journal of Hydrometeorology*, *20*, 1241–1258. https://doi.org/10.1175/jhm-d-18-0242.1

Kramer, P. J., & Boyer, J. S. (1995). *Water relations of plants and soils*. Academic press.

Laio, F., Porporato, A., Ridolfi, L., & Rodriguez-Iturbe, I. (2001). Plants in water-controlled ecosystems: Active role in hydrologic processes and response to water stress: II. Probabilistic soil moisture dynamics. *Advances in Water Resources*, *24*, 707–723. https://doi.org/10.1016/s0309-1708(01)00005-7

Li, W., Migliavacca, M., Forkel, M., Walther, S., Reichstein, M., & Orth, R. (2021). Revisiting global vegetation controls using multi-layer soil moisture. *Geophysical Research Letters*, *48*, e2021GL092856. https://doi.org/10.1029/2021gl092856

Lu, Y., Dong, J., Steele-Dunne, S. C., & van de Giesen, N. (2016). Estimating surface turbulent heat fluxes from land surface temperature and soil moisture observations using the particle batch smoother. *Water Resources Research*, *52*, 9086–9108. https://doi.org/10.1002/2016wr018943

Ma, S., Baldocchi, D., Wolf, S., & Verfaillie, J. (2016). Slow ecosystem responses conditionally regulate annual carbon balance over 15 years in Californian oak-grass savanna. *Agricultural and Forest Meteorology*, *228*, 252–264. https://doi.org/10.1016/j.agrformet.2016.07.016

Mueller, B., & Seneviratne, S. I. (2012). Hot days induced by precipitation deficits at the global scale. *Proceedings of the National Academy of Sciences*, *109*, 12398–12403. https://doi.org/10.1073/pnas.1204330109

Njoku, E. G., & Kong, J. A. (1977). Theory for passive microwave remote sensing of near-surface soil moisture. *Journal of Geophysical Research*, *82*, 3108–3118. https://doi.org/10.1029/jb082i020p03108

Qiu, J., Crow, W. T., Dong, J., & Nearing, G. S. (2020). Model representation of the coupling between evapotranspiration and soil water content at different depths. *Hydrology and Earth System Sciences*, *24*, 581–594. https://doi.org/10.5194/hess-24-581-2020

Qiu, J., Crow, W. T., & Nearing, G. S. (2016). The impact of vertical measurement depth on the information content of soil moisture for latent heat flux estimation. *Journal of Hydrometeorology*, *17*, 2419–2430. https://doi.org/10.1175/jhm-d-16-0044.1

Scott, R. L., Cable, W. L., & Hultine, K. R. (2008). The ecohydrologic significance of hydraulic redistribution in a semiarid savanna. *Water Resources Research*, *44*. https://doi.org/10.1029/2007wr006149

Sehgal, V., Gaur, N., & Mohanty, B. P. (2021a). Global flash drought monitoring using surface soil moisture. *Water Resources Research*, *57*(9), e2021WR029901. 10.1029/2021WR029901

Sehgal, V., Gaur, N., & Mohanty, B. P. (2021b). Global surface soil moisture drydown patterns. *Water Resources Research*, *57*, e2020WR027588. https://doi.org/10.1029/2020wr027588

Seneviratne, S. I., Corti, T., Davin, E. L., Hirschi, M., Jaeger, E. B., Lehner, I., et al. (2010). Investigating soil moisture–climate interactions in a changing climate: A review. *Earth-Science Reviews*, *99*, 125–161. https://doi.org/10.1016/j.earscirev.2010.02.004

Short Gianotti, D. J., Salvucci, G. D., Akbar, R., McColl, K. A., Cuenca, R., & Entekhabi, D. (2019). Landscape water storage and subsurface correlation from satellite surface soil moisture and precipitation observations. *Water Resources Research*, *55*, 9111–9132. https://doi.org/10.1029/2019wr025332

Ulaby, F. T., Batlivala, P. P., & Dobson, M. C. (1978). Microwave backscatter dependence on surface roughness, soil moisture, and soil texture: Part I-bare soil. *IEEE Transactions on Geoscience Electronics*, *16*, 286–295. https://doi.org/10.1109/tge.1978.294586

Wagner, W., Lemoine, G., & Rott, H. (1999). A method for estimating soil moisture from ERS scatterometer and soil data. *Remote Sensing of Environment*, *70*, 191–207. https://doi.org/10.1016/s0034-4257(99)00036-x

Yang, Y., Donohue, R. J., & McVicar, T. R. (2016). Global estimation of effective plant rooting depth: Implications for hydrological modeling. *Water Resources Research*, *52*, 8260–8276. https://doi.org/10.1002/2016wr019392

Yuan, X., Wang, L., Wu, P., Ji, P., Sheffield, J., & Zhang, M. (2019). Anthropogenic shift towards higher risk of flash drought over China. *Nature Communications*, *10*, 1–8. https://doi.org/10.1038/s41467-019-12692-7

Zeng, X. (2001). Global vegetation root distribution for land modeling. *Journal of Hydrometeorology*, *2*, 525–530. https://doi.org/10.1175/1525-7541(2001)002<0525:gvrdfl>2.0.co;2